Performance Assessment of TSO–DSO using Volt-Var Control at Smart-Inverters: Case of Vestfold and Telemark in Norway

Case Study

Victor Astapov
Tallinn University of Technology
Department of Electrical Engineering and Mechatronics
Ehitajate tee 5, Tallinn, Estonia
victor.astapov@taltech.ee

Sergei Trashchenkov
Pskov State University
Institute of Engineering Sciences
L.Tolstoy St., 4, Pskov, Russia
trashchenkov@gmail.com

Francisco Gonzalez-Longatt
University of South-Eastern Norway
Department of Electrical engineering, Information Technology and Cybernetics
Office C224b, Kjølnes Ring 56, 3918, Porsgrunn, Norway
fglongatt@fglongatt.org

Danijel Topic
University of Osijek,
Faculty of Electrical Engineering, Computer Science and Information Technology
Osijek, Croatia
Kneza Trpimira 2b, 31000 Osijek

Abstract *– The massive penetration of distributed energy resources (DERs) in distribution networks provides a strategic opportunity for the distribution system operator (DSO) to coordinate the assets appropriately and offer services to the transmission systems. The IEEE std. 1547-2018 introduced a control mechanism to enable the power electronic converters (PECs) to offer several services, including voltage regulation by controlling the reactive power injection/absorption; this type of PECs is also known as "smart inverter". The participation of the smart-inverters in the voltage regulation with a novel customer-centred piece of legislation and markets provide the DSO with powerful tools to enforce very positive TSO/DSO interactions. This research paper presents a comprehensive assessment of the steady-state performance provided by voltage control at the smart-inverters to the TSO – DSO system. The assessment includes analysing main indicators using time series considering short term (24-hours, 1-minute resolution) and long-term (one-year) horizon. In this paper, the three leading indicators are used as criteria for the assessment: total energy losses voltage profile in the TSO-DSO system and the power flow interaction at the interface between the systems. The assessment is based on numerical results using the DIgSILENT PowerFactory simulation tool, where the voltage controllers have been implemented, and regional electrical system in south-eastern Norway, the area of Vestfold and Telemark as been used for illustrative purposes.*

Keywords*: Ancillary service, control, distribution grid, DG, DSO, PowerFactory, reactive power control, reactive power management, RES, smart inverter, TSO, voltage control.*

1. INTRODUCTION

Electrical power systems are facing many challenges nowadays; one of those challenges is the need to adapt the distributions network to increase the growing integration of renewable-based generation (and storage) at the demand side to allow the customer more active participation in the electricity trade. The old concept of passive and one-directional power flows distribution networks must change. *Distribution system operators* (DSOs) must take advantage of the new interest of customers in installing new low-carbon technologies and the market possibilities of compensating the customer for offering services to the grid. Consequently, the customer-centred active distribution network (ADN) must be flexible and able to adapt, all of the low carbon technologies require power electronic converters (PECs) as interfaces to the grid, such as the case of solar PV (which outputs DC power) or microturbines (high-frequency AC power) [1]. The so-called *power electronic interfaces* (PEI) offer an outstanding instrument to provide controllability features to the DSO; it is particularly true considering the technological advances reached by the development of the smart grids [3], [4].

Modern PEIs are intended to play a crucial role in frequency and voltage control in the ADN, and also, the PEI (when appropriately coordinated) also facili-

tates participation in black start strategies. The IEEE Standard 1547-2018 [5], *IEEE Standard for Interconnection and Interoperability of Distributed Energy Resources with Associated Electric Power Systems Interfaces*, provided a modern way to look at the PEI and allow getting over the limitations of low penetrations of the power converter based *distributed energy resources* (DER) in the electrical networks, and add advanced features on DER, like smart features to *solar PV inverters* [6] and *wind generator inverters* [7]. The IEEE std 1547-2018 [5] created a new tendency in the power electronic converter industry, the so-called "*smart inverter*" [1]. The IEEE 1547-2018 is a crucial enabler to the low carbon technologies in the distribution network, making room for prosumers to offer services to the DSO and then to the *transmission system operator* (TSO) [8].

The smart inverter is a straightforward concept; it is a PEI that is enabled with novel features and functionalities; it is enhanced capabilities, especially the digital architecture, bidirectional communications capability and robust software infrastructure [9], [10].

The IEEE std 1547-2018 and the concept of a smart inverter allows the drawing of the main features of the so-called: *Smart solar photovoltaic inverters*; the features comprise at a minimum the following [8], [11]:

- Voltage ride through
- Frequency ride-through
- Voltage support
- Frequency support, and
- Ramp rates.

The modern IEEE Std. 2030.7, *IEEE Standard for the Specification of Microgrid Controllers* [12], [13] is a crucial document on defining the operation and control so the microgrid; it introduces the fundamental concept of the *Microgrid Energy Management System* (MEMS). In addition, IEEE Std. 2030.7 contains the specifications of the control functions that distinguish the microgrid as a system that can manage itself. Thus, the microgrid (under the concept of IEEE Std. 2030.7) can operate autonomously or grid-connected, seamlessly connect to the utility grid, and enable the microgrid to be disconnected from the utility grid to exchange power supply of ancillary services [14], [15].

The digitalisation of the electricity networks is a reality; the power systems are taking advantage of digital technologies to transform the electricity sector fundamentally. Moreover, the digitalisation of the power systems has cleared the path to overcome barriers (in the past) and allowed a very active and dynamic interaction between TSOs and DSOs.

The increased interaction between DSOs and TSOs can enable better utilisation of DERs -especially at the demand side, increased system flexibility and optimisation of investments in grid infrastructure. However, also, the interactions between TSO - DSO has the potential to overcome several of the traditional problems in electrical networks [11], [13], [16]: relieving congestion of Transmission-Distribution interface (potential to defer infrastructure investment), relief of congestion of transmission lines and distribution lines, fully managed voltage support (TSO↔DSO), balancing challenge, (anti-) Islanding, re-synchronisation & black-start and coordinated protection.

A more adaptive and flexible TSO-DSO operating approach takes advantage of the smart-inverters to provide voltage control of the entire system and take advantage of reactive power/voltage control. The TSO-DSO collaborative approach considered in this scientific paper appropriately employ the smart-inverter installed at the prosumers to provide voltage support to the entire system by adjusting the reactive power injection/absorption at their interface, taking advantage of DGs reactive power capability. The European Grid Code, *Demand and Connection Code* (DCC) [17] established the new distribution systems are requested to have the technical capacity to restrain the reactive power flowing upwards the transmission system at low active power consumption, that is below 25% of their maximal power import capacity [18].

This research paper is dedicated to introducing and assessing the effect of smart inverters voltage control on the quasi-dynamic performance of the TSO – DSO system, considering several time scales [19]. The TSO–DSO system's quasi-dynamic performance assessment is based on two leading indicators; the total energy losses and the voltage profile in the TSO - DSO system. The indicators are calculated from the numerical results obtained in quasi-dynamic simulations using a well-known power system analysis software, DigSILENT PowerFactory. Furthermore, to show the suitability of the proposed approach in a realistic fashion, the assessment in this paper considers the regional electrical system of Vestfold and Telemark, located in the south-eastern part of Norway. This scientific paper is structured in five sections. Section II presents the primary voltage-control operating mode of the smart inverter; Section III is focused on establishing the critical aspects of TSO-DSO modelling. Section IV is dedicated to assessing the impact of voltage control of smart-inverters in multi-time scale quasi-dynamic performance of the TSO – DSO regional system of Vestfold and Telemark, Norway. Finally, this scientific paper closes with Section V presenting the main conclusions and findings. One main contribution of this paper is making evident that reaching the minimum total energy losses implies a compromise between the TSO/DSO losses; as a consequence, enabling the interaction TSO/DSO that reaches a global benefit for all parties requires sub-optimum losses at each individual system.

2. VOLT-VAR CONTROL IN SMART CONVERTERS

Voltage control in a traditional transmission system is reached by several mechanisms where the provision/consumption of reactive power is the central con-

trol element. Some of the mechanism used in voltage control in traditional transmission includes the use of power transformers equipped with an *on-load tap changer* (OLTC). The scientific literature is rich in many other classical Volt-var control when dealing with voltage control at transmission-level [20-22]: shunt capacitors/reactors, transformer tap changers, synchronous generators, synchronous condensers, FACTS, e.g., STATCOM, SVC and HVDC. The voltage control at the distribution network uses several reactive power sources/control [23], [24] such as voltage regulators, transformer tap changers, shunt capacitors. The power utilities included in the grid code specific connection requirements generation units, and those requirements vary from country to country, installed capacity and the voltage level of connection, and some other factors.

The smart-inverter concept allows the power-converter based distributed energy resources (DER) units to produce/absorb reactive power depending on a control rule that can be defined in many ways. For instance, the smart inverter working in control mode can adjust the operating power factor to absorb reactive power at the controlled point to bring the high voltage down within standard limits and inject reactive power to increase voltage level, which consequently changes reactive power flow in the grid. A vital element of the modern voltage control aforementioned is that nowadays, the controlled node is not necessarily the connection point of the DER unit. It can also be a common coupling point (PCC), a boundary between TSO and DSO, or a specific node in the grid. The inclusion of digital communication technologies basically reaches the flexibility in the location of the control node. Today the additional regulation types such as constant voltage (const *U*), constant power factor (const cos φ), *Q*(*P*), or *P*(*U*) is not a rarity, especially for high capacity (multi-MW) DG. For example, a DER in the low voltage network in Germany must implement at least one of those voltage control functions [25], [26].

The explanation of such control methods is widely presented in many scientific publications [27-29] , but the authors would like to highlight a few key points relevant to the control strategies used in this paper and how they are implemented in the power systems simulation environment. The technological advances on PEC and the new IEEE std 1547-2018 makes the smart-inverter a desirable solution to provide Volt-var control and positively impact the distribution systems. Smart-inverter supports the following control modes, which are considered in the paper: (i) Constant reactive power, (ii) Constant voltage, (iii) Voltage Q-droop, (iv) Q(U)-Characteristic (see Fig. 1), and the control can be implemented locally and remotely. Technically ii-iv modes are pretty similar, despite that constant voltage controller implementation does not have a deadband and is accordingly stricter. In such mode, reactive power fluctuations are more often compared to (iii) and (iv).

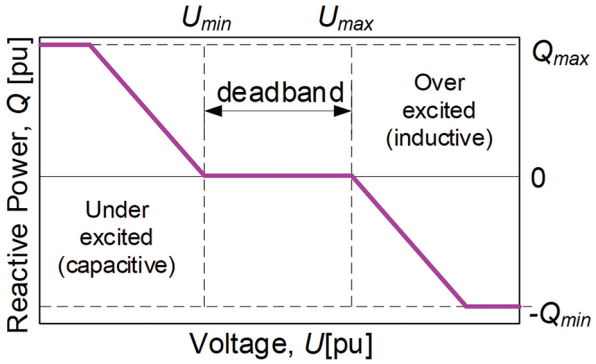

Fig. 1 Illustrative representation of the *Q*(*U*)-characteristic

As mentioned before, the model includes the possibility of controlling parameters locally and at some specific point in the network. In this paper, the point of control is the boundary between TSO and DSO networks. The so-called wide-area control is basically a centralised controller that takes measurements and then, using a predefined control rule, defines the operational setpoints of the smart-inverters. Depending on the control model defined, the following parameters should be set up: reactive power setpoint (operation considering constant power factor); voltage setpoint u_{setp} and reactive droop Q_{droop} in Mvar/pu (operation considering constant voltage). The wide-area control use measurement devices located a the branch or boundary where the controller is intended to fulfil the control rule. The voltage setpoint is modified depending on the reactive power flow at the Q-measurement point as follows:

$$U'_{setp} = U_{setp} + \frac{Q_{meas}}{Q_{droop}} \tag{1}$$

where: U_{setp} is the voltage set point in pu. of the busbar, U'_{step} represents the voltage set point in pu., including the droop characteristic, and Q_{meas} and Q_{droop} are the measured reactive power in Mvar and droop in Mvar/pu, respectively.

Moreover, for station control contribution of the different reactive power sources to the control of the voltage is specified. Every source is assigned a contribution factor (K_p) that indicates the percentage to feed an actual value, in addition to its set point. This factor is calculated according to five different options, including dispatched active power, individual reactive power, or the rated power as in our case.

During the operation, especially in remote control, demands for reactive power could be outside the invertor capability limits. Another boundary is derived by the attributes of most inverters, which are not able to provide reactive power outside of the feed-in periods. Inverters with called "*Q* at night" option are not considered in this paper. On the other hand, the smart-inverters in this paper are enabled with a reactive power characteristic that includes the voltage dependence; the implemented curve is depicted in Fig. 2.

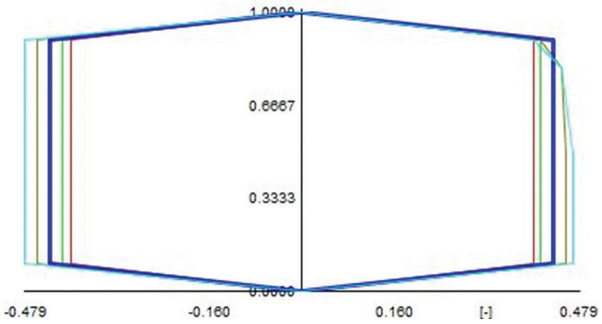

Fig. 2 Example of a reactive curve of a smart-inverter used in a PV system, considering voltage dependence.

3. MODELLING AND SIMULATION DESCRIPTION

The performance of voltage control mechanisms in smart-inverters and releasing the synergy between TSO/DSO systems considering the paradigm of tied-micro grids is presented in this paper considering an illustrative case of a TSO-DSO. The main interest is the performance of the voltage control mechanism in the quasi-dynamic voltage profile of the regional TSO-DO power networks in the South-Eastern part of Norway. The equivalent TSO consists of a detailed high-level representation of the regional 132-kV system, Telemark and Vestfold area [11], [30]. The DSO network is created [11] in order to represent the main feature of the 11 kV distribution system. This section is dedicated to modelling aspects of the TSO-DSO. More details on the TSO-DSO system can be found at [11], [31].

Transmission System Operator (TSO)

A detailed high-level model of the regional TSO network of the south-eastern area of Norway, specifically Vestfold and Telemark, is used in this paper. Using information publicly available, the network model has been created. The single line diagram of the TSO model of the Vestfold and Telemark area in Norway is depicted in Fig. 3 [10]; the network model includes seven synchronous generators (SGs) representative of the regional hydropower plants locally available in the Vestfold and Telemark area. The authors have included the connections to the National transmission system in Norway as a simplified equivalent model at 300 and 420 kV levels.

Distribution System Operator (DSO)

The authors have created a representative substation of the local DSO at the region of Telemark and Vestfold; it is used for performance analysis in this paper and can be extended and generalised. The distribution substation is modelled considering a classical step-down transformer (110/11 kV) and a typical 11 kV distribution feeder (representative of the south-eastern part of Norway), as this voltage level is the most widely used voltage level in the Telemark area, Norway.

Underground cables mostly dominate the Norwegian distribution networks in urban areas, and it is usually built like a meshed network. The distribution net-

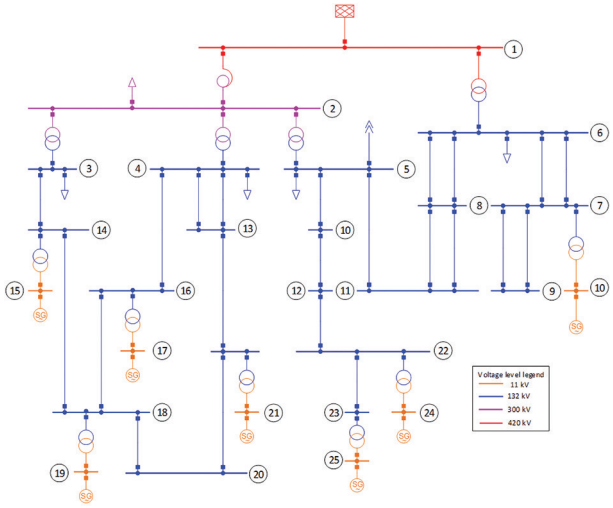

Fig. 3. Single line diagram of the TSO system implemented in this paper: It is a representative of the regional transmission system of Vestfold and Telemark at 132, 300 and 420 kV [11].

works in Norway are built in a meshed configuration, but it is operated as a radial configuration to make it easier to control and predict the different currents and voltages in the grid. Consequently, the authors decided to consider the representative Norwegian distribution feeder as a radial topology, as shown in Fig. 4; however, the feeders are equipped and designed so that it will be possible to work in a ring topology (no considered in this paper). For simplicity, the distribution grid consists of fourteen feeders, three feeders have been modelled in full detail, and the remaining eleven feeders are presented as an equivalent lumped system.

The proposed DSO network has been enhanced with the integration of smart inverters, making the DSO network an active distribution network. Consequently, the DSO system has been intentionally selected to resemble a specific part of the city of Skien in the Telemark area, Norway. The local company Skagerak Nett provides the electricity service as the city of Skien, and the company owns and operates a solar-powered microgrid (solar rooftop panels 800 kW), including a battery energy storage system (BESS, 800kW/1000 kWh). The micro-grid is called Skagerak Energilab, it is supposed to be dedicated to research and development activities, and it is located at the Skagerak Arena, with a potential peak-load of 1,000 kW during football matches. The model used to emulate the performance of the Skagerak Energilab has been created by the authors using information publicly available; the Energilab is equipped with smart-inverters where the voltage control and reactive power production are enabled, and the model is integrated at bus 4 of the feeder 3 to at Fig. 4.

Load and generation profiles

The distribution substation used to emulate the DSO system at node 5 has a 30 MVA capacity; the load has equally divided between 14 feeders. A nominal load

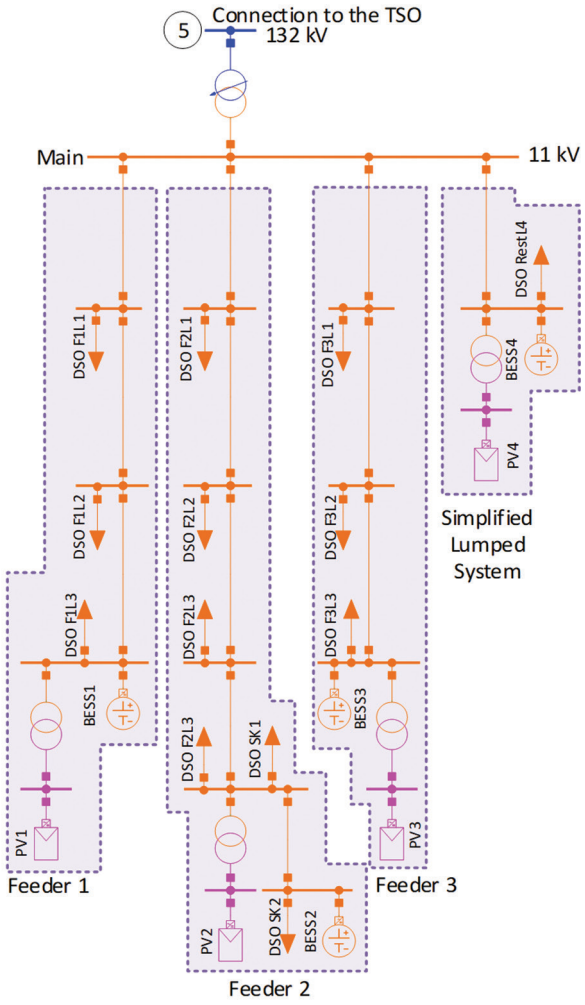

Fig. 4. Single line diagram of the DSO system implemented in this paper: Representative substation at Vestfold Telemark, considering four radial feeders and PV and BESS are depicted for future simulation scenarios [11].

demand of 2 MW is used at each one of the feeders. This way, Feeder 4, which represents simplified 11 feeders, has a peak load of 22 MW.

The total load of the DSO system is considered a residential load except for the case of the Skagerak Energilab, which is considered a special load. Load profiles representative of the 24-hour operation of the loads is synthetically created [32], [33] by using the tool developed by the Centre for Renewable Energy Systems Technology (CREST) at Loughborough University in the United Kingdom.

The CREST model was modified [11] to represent the Norwegian consumer's weather and load. The CREST model was originally created based on stochastic models of British or Indish power consumers. The CREST model was improved and enhanced to consider realistic location in Norway by using the temperatures in Skien, Norway. Also, the original CREST model considers gas as the primary source of heating inside the dwelling, as that is the primary energy source for heating in Great Britain. Therefore, the CREST model is modified to represent the reality of primary resource use for heating in Norway, mainly done by electricity. Fig. 5 shows the 24-hour load profile (1 sample per minute) of loads 1, 2 and 3 connected at the feeders 1 to 3.

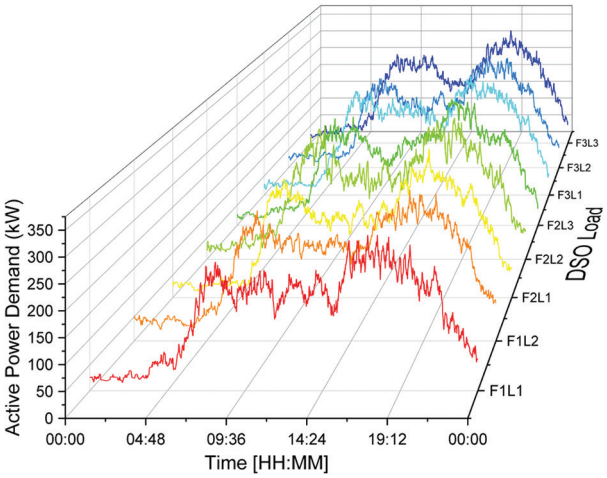

Fig. 5. Hourly power demand (in kW) several loads of the DSO.

Identical electrical consumption patterns in two dwellings have an extremely low probability; consequently, it is required to calculate several consumption profiles for several dwellings to the extent that it is possible to reach the wanted peak load for the different loads in the DIgSILENT PowerFactory quasi-dynamic model. Therefore, the load simulations will be performed individually for all the various loads in the model so that none of the loads will have an identical pattern or peak load.

The DSO Feeder 4 is a typical distribution feeder considering a total combined demand of 22 MW, considering residential loads, and using the modified CREST model, the synthetic data of a local residential area with least 6.300 dwellings was created for a load profile of 24-hour (1-minute resolution), and the profile is shown in Fig. 6.

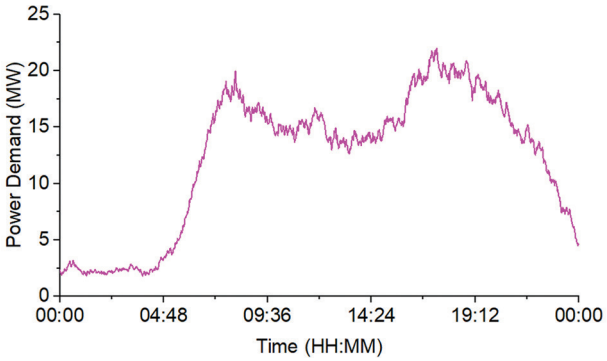

Fig. 6. Hourly load profile for the 22 MW load (1 sample per minute).

To extend the time scale, the diversity of the loads was accordingly modified considering the power demand in the whole system during the year; the authors added additional profiles parameters considering standardised

load profiles. The adjusted profiles include characteristics patterns considering different seasons, working days, and weekends. It allowed producing synthetic data for a whole year loads based on the 24-h profile created by the modified CREST model. By assigning three different profiles to 12 different loads produced a more realistic total load profile avoiding unrealistic simultaneous load peaks. Based on that, the load profile presented in Fig. 5 can be observed as DSO_F1L1 load in summer days (Friday-Sunday) on Fig. 7, which has different peaks and is slightly reduced compared to winter where loads are maximum.

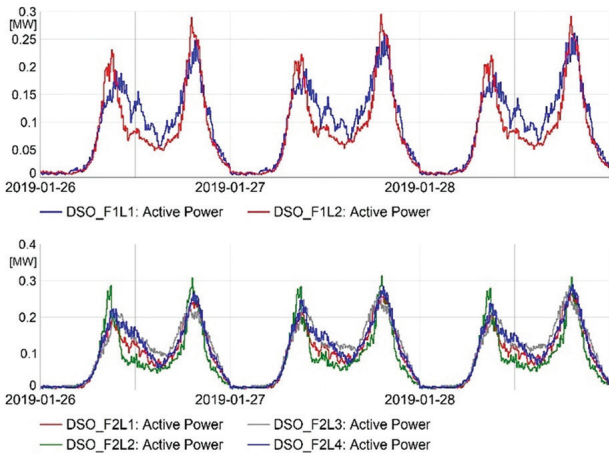

Fig. 7. The implementation of time characteristics for DSO loads.

For TSO loads, time characteristics were implemented the same way as for DSO but based on peak power instead of the day-hourly profile, as it was shown in Fig. 8.

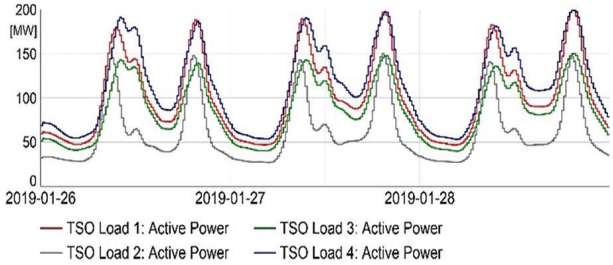

Fig. 8. The implementation of time characteristics for DSO loads

Special Load: Skagerak Arena

The Feeder 2 includes the correction of the Skagerak Arena, which is a stadium dedicated to the local football team [34], [35]. It is collected from publicly available data that the Skagerak Arena have a potential peak-load of 1,000 kW during football matches. The total power demand is divided between two distribution transformers; one transformer supplies around 300 kW (for daily consumption), and the second one is 700 kW (Mainly for the floodlights during football matches). Therefore, the remaining load of this feeder will be around 1.000 kW, which will be divided between three loads of a little over 300 kW.

The implementation of time characteristics applied for general DSO loads is not applicable for Skagerak Arena since matches and events obviously do not occur here every day. Therefore, the authors created and implemented characteristics based only on weekdays. The weekly pattern for Arena is as follows: on Sundays, the Arena is fully loaded with a peak-load of 700 kW; on Saturdays, it is partly loaded for pre-match events with 10% scaling, and on other days it consumes only 1% of load demands. The implementation of discrete-time characteristics for Arena (DSO_SK1 and DSO_SK2) is presented in Fig. 9.

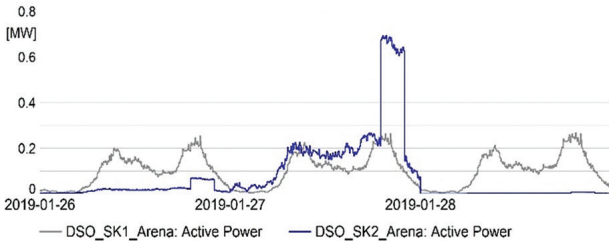

Fig. 9. The implementation of time characteristics for Skagerak Arena loads.

Modelling of BESS

The appropriate control of a BESS provides the possibility of injecting/absorbing active/reactive power, thus providing support to the TSO-DSO interactions. In this scientific paper, the authors have taken advantage of the quasi-dynamic simulation language (QDSL) to create a simplified model of a BESS inside the power system simulation environment. The BESS model aims to simulate the operation of the set, battery, voltage control, and charge control based on the feedback of signals taken from the network operation. The BESS model has been enabled with a simple state of charge (SOC) controller; it controls the active power injection/consumption to keep the battery between the operational limits (SOC_{min}, SOC_{max}). The battery has been modelled considering a simple equivalent circuit model considering the number of individual cells (series and parallel) in the pack and where the SOC is calculated based on the changes of the energy absorbed/produced based on the rate of charging/discharging current.

Performance Indicators

The following data for analysis were obtained during simulations, such as power flow, maximum generation and loads, line loading, and voltage fluctuations. However, for the evaluation of each control mode, we decided to select criteria as follows:

- Total energy loss (MWh) in the DSO and TSO networks.
- Voltage improvement (Voltage difference, min and max values).
- Reactive power flow via DSO/TSO (considered for year scenarios).

- The total active and reactive power production of the distributed energy resources.

Such indicators are general measurements or values that have a relevant impact on a specific study case. In the case of efficiency and Volt-var control, the indicators used to assess the performance of the TSO-DSO system are shown in the following subsections.

Energy loss (E_{loss})

Energy loss has a financial impact on the total operating cost. As a consequence, in this paper, the total energy loss (MWh) in one day is used as an index to assess the quasi-dynamic performance of electricity TSO-DSO interactions. The total energy loss (E_{loss}) is calculated by using the following formula [36]:

$$E_{loss}\left[\frac{MWh}{day}\right]=\int_{t=00:00}^{t=24:00}P_{loss}(t)dt \tag{2}$$

Therefore, the afore presented equation is discretised over a 24-hour:

$$E_{loss}\left[\frac{MWh}{day}\right]=\frac{1}{60}\left[\frac{h}{\min}\right]\sum_{t=0}^{\frac{\min}{day}}P_{loss,t} \tag{3}$$

Voltage Difference (VD)

The index maximum *voltage difference* (VD_{max}) is used in this paper to relate the lowest voltage level (U_{low}) and the highest voltage level (U_{high}) during a period of 24-hours. The voltage difference (*VD*) of these is compared to the no-load voltage ($V_{no\text{-}load}$); therefore, the *VD* is expressed in percentage (%) is defined as:

$$VD\left[\%\right]=\frac{VD_{\max}\left[V\right]}{U_{no-load}\left[V\right]}\times 100\% \tag{4}$$

$$VD_{\max}\left[V\right]=U_{high}\left[V\right]-U_{low}\left[V\right] \tag{5}$$

Reactive power flow via TSO/DSO boundary

Reactive power flow has been disregarded for many years in electrical power systems because electricity networks are designed to transmit active power, as that is the energy source billed by the utilities. On the other hand, voltage variability and control has been perceived as a local problem that typically is solved by a local source of reactive power or voltage control. However, the proliferation of smart-inverters in the distribution network has changed the old paradigm, and local reactive power control has to help improve the whole system's performance. Up to now, no reactive power market is enforced commercially around the world, but time-based marked defined prices would be a game-changer for the customers regarding the location of reactive power production. In this paper, the reactive power flows between the DSO and TSO are quantified by measurements devices at the interface between the systems (Q_{ij}).

Annual Energy production (E_{PDG})

A customer centred market might motivate the owner of the distributed resources located at the demand side to participate in the energy trade on that market; as a consequence, the annual energy production arises an important indicator at the distributed resource assets installed at the DSO. The annual energy production of distributed resources installed in the DSO, e.g., BESS and PV, are calculated (E_{DER}) are calculated. It helps to make evident the performance of the controller assesses at the time to show the operation patterns of the distributed energy resources. The annual energy production is calculated in the separated fashion of the active (E_{PDER}) and reactive power and calculated as:

$$E_{PDER}\left[\frac{MWh}{year}\right]=\int_{t=0}^{t=8760}P_{DER}(t)dt \tag{6}$$

$$E_{QDER}\left[\frac{M\,\mathrm{var}\,h}{year}\right]=\int_{t=0}^{t=8760}Q_{DER}(t)dt \tag{7}$$

where $P_{DER}(t)$ and $Q_{DER}(t)$ are the instantaneous active and reactive power production, respectively.

Simulation Scenarios

The performance assessment of TSO–DSO interactions in Vestfold and Telemark considering the Volt-Var control at smart-inverters in the case of is assessed in two main general scenarios:

- **Short-term variations (ST):** the main performance indicators are assessed over a short-term period, 24-h profile. This assessment is specifically designed to observe and identify intra-hour patterns of variations.
- **Long-term variations (LT):** A long term horizon of simulation is used to analyse extra-day patterns. Mainly, a 365-day period is used in this scenario.

The following subsections are specifically designed to present simulation results and discuss in detail the main findings.

4. SHORT-TERM (S.T) PERFORMANCE ASSESSMENT

Scenario ST.I: Base

The base scenario is used to assess the performance of the TSO/DSO system, considering a typical traditional system where there is no integration of low carbon technologies at the distribution network. This scenario is called the base and used as a reference for comparison with other scenarios. Table 1 shows a summary of the energy losses share between TSO and DSO during the 24-hour and the voltage difference indicator. A plot of 24-hour active power losses at the TSO/DSO is pre-

sented in Fig. 6; it is essential to notice that the maximum losses at the DSO system are related to times of the peak demand (08:00 and 17:30, see Fig. 10).

Table 1. Energy losses and voltage differences: Scenario ST.I

System	Energy losses E_{loss} [MWh/day]	Voltage difference UD [%]
TSO-grid	194.81	2.17
DSO-grid	1.820	1.88

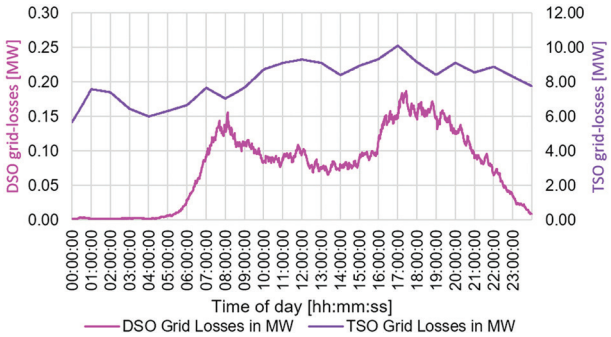

Fig. 10. Plot of the active power losses (MW) at the TSO/DSO systems during a period of 24-hours.

Scenario ST.II: Integration of Top Roof PV

This scenario, the TSO/DSO network is as described in Scenario I, but now it considers the integration of PV systems at the residential level, the so-called top roof PV system populated at the demand side. The top roof PV system consists of several PV panels located at the property's roof and a smart inverter installed inside the property. This scenario does not consider the use of energy storage; consequently, the PV locally produce electricity during sunlight hours, and then the customer must buy electricity during off-daylight hours.

In this paper, the top roof PV model was set up to duplicate the conditions at the location named Falkum, in the city of Skien, south-eastern part of Norway (precisely, 59.2° latitude, 9.6° longitude). The PV system considers 160W/35V solar panels, considering single crystalline silicon. This scenario is designed to consider a complete integration of the PV system in the DSO network. Ideally, the total installed capacity of the top roof PV system is adjusted to be above the peak of the local demand; Table 2 depicts a summary of the DSO performance integrating top roof PV at each one of the feeders and the total DSO grid.

The smart-inverters allows the top roof PV system to fed reactive power (when operates as over-excited), and absorbing reactive power (when operates as under-excited) allows the smart-inverter to control the voltage by changes of reactive power. This scenario considers a full DSO operating the distribution network; as a consequence, the DSO authorises the active participation of the smart-inverter in voltage regulation. This paper considers six different voltage control methods, and their specific details are presented in Table 3.

Table 2. Summary of the Integration of PV systems in the DSO System.

Feeder	Total installed Power [kWp]	Number of panels	Penetration level [%]
1	2,000	12,500	100.6
2	840	5,250	45.4
3	2,000	12,500	105.5
4	22,000	137,500	110.5
Total DSO-grid	**26,840**	**167,750**	**104.6**

Table 3. Details of voltage control implemented at the smart-inverters: Scenario ST.II.

Case	Description
1	Constant power factor, *pf* = 1.0 (no reactive power support)
2	Constant power factor, *pf* = 0.95
3	Constant power factor, *pf* = 0.90
4	Slow voltage droop: *Q(U)* – 30 % Droop set to K_U = 30 %, U_{set} = 1.0 pu
5	Fast voltage droop: *Q(U)* = 10 % Droop set to K_U = 10 %, U_{set} = 1.0 pu
6	Constant voltage set-point at U_{set} =1.0 pu

Two important considerations are taken into account when operating the smart-inverters: (i) the inverters deliver all the active power produced by the PV systems at the time, (ii) the inverters are equipped with voltage control that enables the reactive power injection/absorption. Fig. 11 depicts an outline of the numerical results of total energy losses [MWh/day]. It is clear from the figures that the smart-inverter operating in voltage support control mode provides a reduction in the total power losses and produces a positive change in the voltage profile of the whole TSO-DSO system.

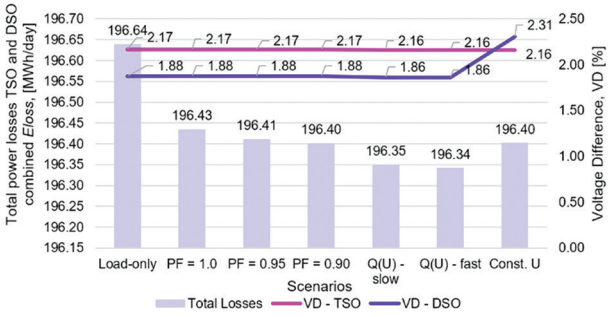

Fig. 11. Summary results of different voltage control implemented at the smart-inverters: Scenario ST.II.

The numerical results of the quasi-dynamic simulation over a 24-hour period show that the most significant and most minor total energy loss (E_{loss}) are found when the voltage controller is adjusted to the fast droop settings (Case 5, see Table 3) and power factor equal to 1.0 (Case 1, see Table 3), respectively.

The energy-saving of TSO and DSO is calculated referred to the Scenario ST.I (load-only) results are shown in Table 4. One essential element here is the most considerable energy reduction of TSO using Case 6. Meanwhile, the most significant energy reduction of DSO occurs using Case 4. The maximum TSO/DSO saving occurs at Case 5 (*Q*(*U*) fast), but the savings at this situation the energy saving is not maximum at each system.

Table 4. Energy savings of cases comparison based to Scenario ST.I (load-only): Scenario ST.II.

Scenario ST.II Case	Energy-saving TSO [MWh/day]	Energy-saving DSO [MWh/day]	Energy-saving Total [MWh/day]
1	57.1	147.1	204.2
2	73.4	154.7	228.0
3	80.8	157.0	237.9
4	131.4	157.8	289.1
5	171.0	126.0	297.0
6	220.0	17.0	237.0

Scenario ST.III: Integration of PV and BESS

In this paper, the previous analysis is taken as a reference to define simulation scenarios considering the integration of BESSs into the DSO. In this specific case, the two extreme cases of the Scenario ST.II (PV-voltage controllers) are selected as the baseline of the cases considering the integration of BESS in the DSO network; Table 5 is used to summarise the set of simulation cases considered in this paper.

Table 5. Details of voltage control implemented at the smart-inverters: Scenario ST.III.

PV-system controller scenario	Case	BESS controller scenario
Scenario ST.III.A Lowest losses: *Q*(*U*), K_U = 10 % *Scenario II, Case 5*	1	Power factor, *pf* = 1.0
	2	Power factor, *pf* = 0.9
	3	Slow voltage droop: *Q*(*U*) = 30 % Droop set to K_U = 30 %, U_{set} = 1.0 pu
	4	Fast voltage droop: *Q*(*U*) = 10 % Droop set to K_U = 10 %, U_{set} = 1.0 pu
	5	Constant voltage setpoint
Scenario ST.III.B Highest losses *pf* = 1.0 *Scenario II, Case 1*	1	Constant power factor, *pf* = 1.0
	2	Constant power factor, *pf* = 0.9
	3	Slow voltage droop: *Q*(*U*) = 30 % Droop set to K_U = 30 %, U_{set} = 1.0 pu
	4	Fast voltage droop: *Q*(*U*) = 10 % Droop set to K_U = 10 %, U_{set} = 1.0 pu
	5	Constant voltage setpoint

Scenario ST.III.A: Lowest PV-losses scenarios

This scenario is created to assess the performance of the PV smart-inverters enabled with controllers set to *Q(V)* operating mode and K_v = 10 %; consequently, the lowest losses caused by the PV integration are considered. Five different cases are considered in the assessment regarding the voltage control at the smart-inverter installed at the BESSs. Fig. 12 depicts the performance of the energy losses (E_{loss}) and voltage differences (*VD* in percentage) during a 24-hour period. It is observed from the numerical results that the combined minimum energy losses are found when the *Q*(*U*)-fast control is enabled in the smart inverters (Case 6).

Scenario ST.III.B: Highest PV-losses scenarios

This scenario is designed to assess the performance of the highest losses caused by the PV system when the smart inverters are enabled with a voltage controller that follows a constant power factor of 1.0; the BESS is alternatively assessed considering five cases of voltage control at the smart-inverter. Fig. 13 shows the numerical results of the energy losses (E_{loss}) and voltage differences (*VD*) during a period of 24-hours. The lowest combined minimum energy loses are found when the controller of the smart-inverters is operating at constant voltage but tends to produce higher voltage levels at the DSO network.

Summary of Scenario ST.III

Table 6 shows a complete summary of the numerical results of the simulations considering the different scenarios where the controllers are enabled ta the smart-inverters. The table has been formatted using a colour-based scale, where the green colour represents the most beneficial result for an indicator and the red colours the least beneficial.

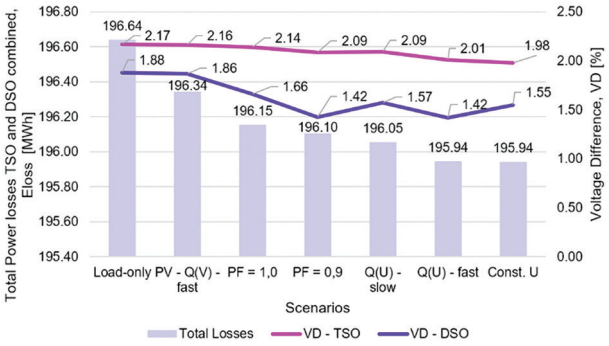

Fig. 12. Summary results of different voltage control implemented at the smart-inverters: Scenario ST. III.A.

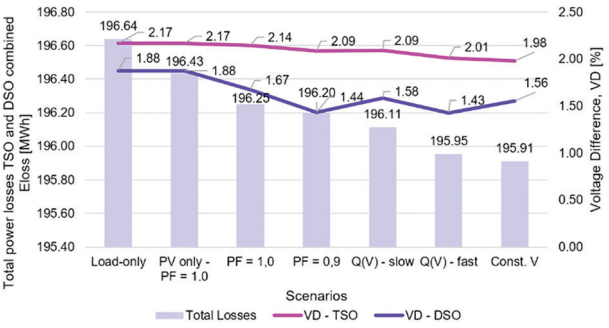

Fig. 13. Summary results of different voltage control implemented at the smart-inverters: Scenario ST.III.B.

The summary presented in Table 6 allows concluding that for the DSO-TSO case shown in this paper, an excellent performance with respect to both energy losses and voltage difference in the DSO-grid is reached when the smart-inverter at the PV system operating at unity power factor and the voltage controller of the BESS inverter set to $Q(U)$, $K_U = 10$ %.

Furthermore, those scenarios show a lower-than-average voltage difference and energy losses in the TSO-grid, as a consequence, it making it one of the most efficient scenarios concerning total energy loss.

5. LONG-TERM (L.T) PERFORMANCE ASSESSMENT

A comparison of the initial 24-hour performance of the TSO-DSO model considering the implementation of BESS and installation of top roof PV modules was described in [11]. The examination period was based on the whole 24-hour period. In this paper, the performance assessment extends the simulation period up to an entire year (365-day). The following subsections are dedicated to assessing the performance of the TSO-DSO interactions, including several operational scenarios for the investigated grid. Few of them are enhanced from [11] to include long-term variation over a period of a year.

Table 6. Summary of the simulation results with BESS scenarios.

PV - Setting	BESS - Setting	VD - DSO	VD - TSO	DSO E_{loss} [MWh/day]	TSO E_{loss} [MWh/day]	Total E_{loss} [MWh/day]
Scenario ST.III.A	1	1.67	2.14	1.52	194.73	196.08
	2	1.44	2.09	1.50	194.70	196.20
	3	1.58	2.09	1.47	194.64	196.11
	4	1.43	2.01	1.47	194.48	195.95
	5	1.56	1.98	1.54	194.37	195.75
Scenario ST.III.B	1	1.66	2.14	1.52	194.63	195.99
	2	1.42	2.09	1.50	194.60	196.10
	2	1.57	2.09	1.51	194.54	196.05
	4	1.42	2.01	1.54	194.40	195.94
	5	1.55	1.98	1.65	194.29	195.84

Scenario LT.I: Base

The first simulation scenario represents TSO-DSO network, considering there is not the integration of smart-inverters at the distributed energy resources, PV and BESS; this scenario replicated the short-term scenario ST-I but considers a long term simulation horizon (1-year).

Scenario LT.II: Unity power factor

The smart-inverters installed at the DSO are controlled using constant reactive power operating mode where the reactive power is controlled to maintain a unity power factor at the time that reduces peaks, load flow and cable loading; as a consequence, the top roof PV system and the and BESS are operating in such way. Fig. 14 illustrated the case of node 3, Feeder 3.

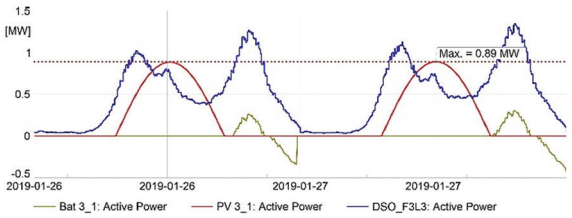

Fig. 14. Illustrative example of active power flow at the distribution line and the BESS active power production showing the peak shaving operation (highlighted in red colour).

It is easy to see the peak shaving capability of the enabled controller at the BESS. The black line at the figure depicts the actual power, and the blue line is dedicated to the performance without BESS. In other words, instead of loading the distribution line and transferring more than 1 MW, the controller enabled BESS to generate around 200 kW to supply load DSO_F3L3. Fig. 15 represents the operation of PV BESS system at feeder 3, and the profile of load DSO_F3L3, which is connected to the same node.

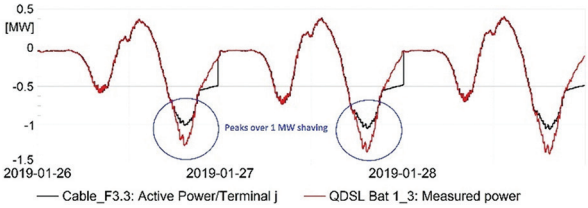

Fig. 15. Illustrative example of operation of distributed energy assets (BESS-PV) connected at the feeder F3 in Scenario LT.II

Scenario LT.III: mixed control strategies

Results of the 24-hour simulation showed that the smart-inverter at the PV system operating $pf = 1.0$ and the voltage controller of the BESS inverter set to $Q(U)$, Ku = 10 % has excellent performance with respect to both energy losses and voltage difference in the DSO-grid. Fig 16 shows the simulation results of the operation of PV-BESS pair considering the unity power factor ($Q = 0$) and $Q(U)$ control, $K_u = 10$ %. In this case, the top roof PV system keeps reactive power as zero (as expected by the operation mode, const $Q = 0$), BESS injects reactive power according to the voltage measurements and $Q(U)$ settings.

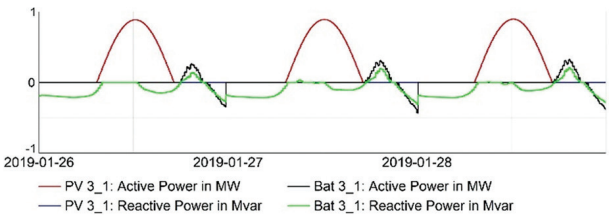

Fig. 16. Illustrative example of the operation of BESS-PV system at the DSO feeder F3 in Scenario LT.III

Scenario LT.IV: Wide area voltage control

This operation scenario is characterised by the implementation of a wide area voltage control with the main

objective of monitoring and controlling the interactions at the TSO/DSO boundary. In this case, the voltage controller is designed to keep the steady-state voltage at PCC at a predefined setpoint ($|U_{set}|$ = 1.00 pu), the action control is taken in the relative power injection/consumption of the BESS as follow: if the voltage is below the setpoint, PV and BESS system inject reactive power and opposite: when is overvoltage. Fig 17 shows the performance of the wide-area voltage controller over a period of three days, and there is a clear correlation between the voltage and reactive power as defined by the controllers. It is possible to see that during periods where the voltage drops below the setpoint ($|U_{set}|$ = 1.00 pu in this case), either PV or BESS are injecting reactive power. Usually, during daylight, reactive power is provided by PV; during the night by BESS. Results were obtained with the setting of 100 MVAr per pu (1 MVAr for 1.0% droop).

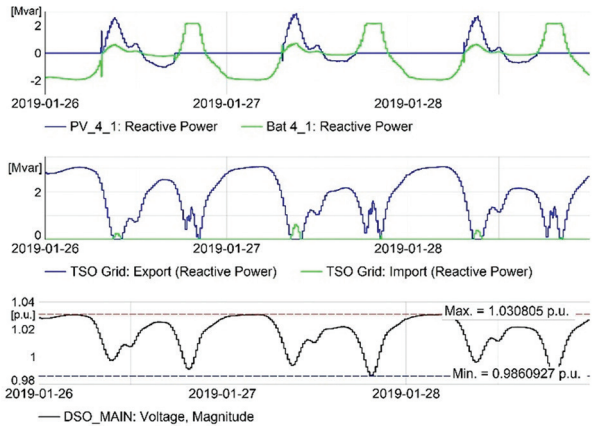

Fig. 17. The operation of BESS-PV system at the feeder F4 in Scenario LT.IV

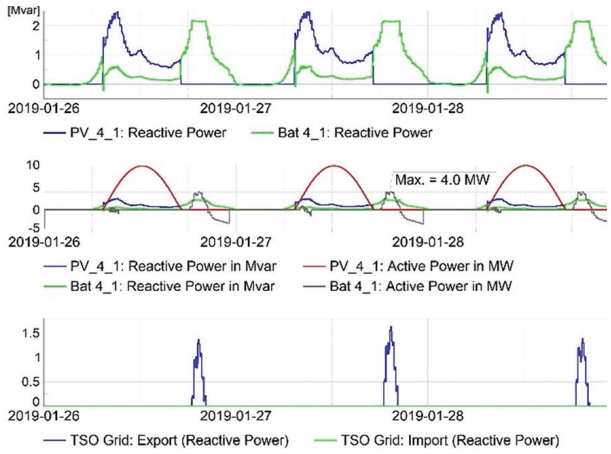

Fig. 18. Illustrative example of the operation of BESS-PV system at the feeder F4 in Scenario LT.V

Scenario LT.V: Wide area reactive power control

In this scenario, smart-inverters of PV and BESS aimed to keep reactive power flow via TSO/DSO boundary as zero (Q = 0 pu). From Fig. 18, it can see that most of the time, it is possible to achieve. However, the observed peaks of reactive power interchange can be explained that PV inverters cannot inject reactive power when there is no active power output. The BESS inverters cannot inject reactive power when SOC is low and requirements (settings) for reactive power injection are not fulfilled.

Results of Scenario LT.III

For each one of the long term (LT) operational scenario one-year simulations were made with the recording results for PV, BESS systems, DSO and TSO separately with the aim to obtain values of annual energy production and losses, active and reactive power flow via TSO/DSO boundaries maximum and minimum values for voltage. The most significant results are illustrated in Fig. 19 – Fig. 21.

Fig. 19 shows the reactive power production/consumption of the distributed energy resources, e.g., PV and BESS, during a period of one year, and the same figure shows the instantaneous active power losses (P_{loss}, MW) and energy loss in the DSO network (E_{loss}).

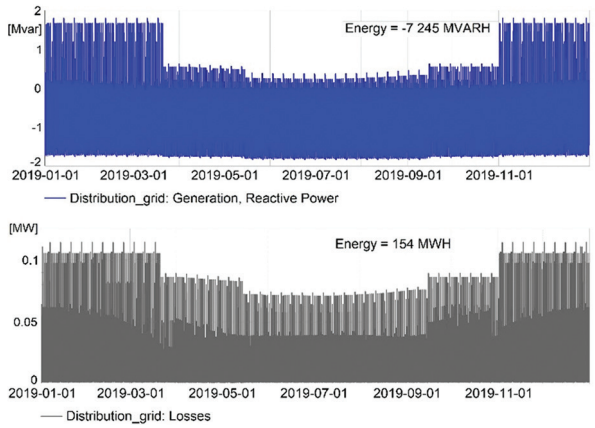

Fig.19. Illustrative example of the operation of DSO in the case of Scenario LT.III.

Fig. 20 shows the performance of voltage profile as measured at the boundary between the TSO-DSO networks (also known as PCC) and the minimum and maximum values during one year. The bottom part of Fig 21 shows the performance of the reactive power flow at TSO/DSO boundary discriminating the import/exports conditions created by the reactive power management control system (station controller).

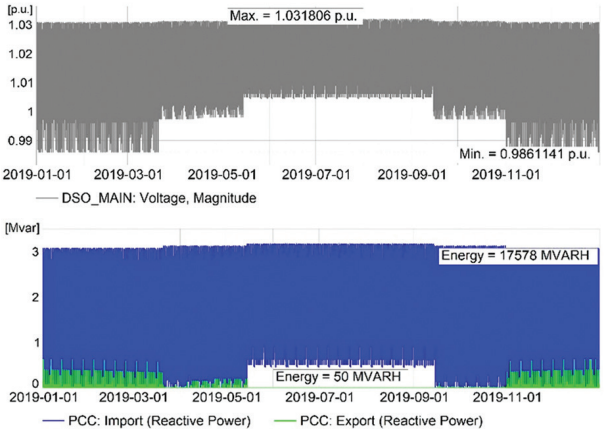

Fig. 20. Results for DSO in Scenario LT.IV (remote const U).

Fig 21 shows the performance of the reactive power flow via TSO/DSO boundary where the power flow is reduced by the control actions taken by the controller at the time the figure depicts the performance of the PCC steady-state voltage, indicating how voltage profile is changed in such operational scenario.

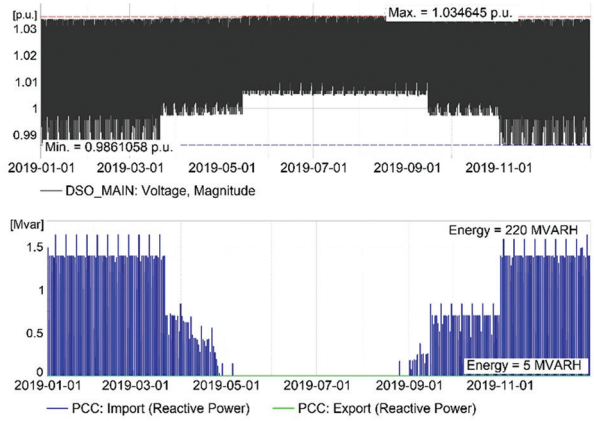

Fig. 21. Results at TSO/DSO boundary in case of Scenario LT.V

A summary of the main indicator used to assed the long term performance of the operating scenarios is shown in Table 7. The summary provided a clear comparison between operational scenarios taking into account indicators mentioned in section 4.

Using the scenario LT.I, as a reference, the integration of the distributed energy resources (PV and BESS) -LT.II- provided a smooth voltage provide and reduction in extreme voltages when the TSO-DSO losses are reduced. The ST.III with the implementation of settings taken from LT.III, system performance increased: voltage fluctuations and losses reduced when compare to ST.II.

The scenario LT.IV aims to control voltage at the controlled node. As a consequence, there is an apparent reduction in voltage fluctuations. However, since the voltage control is performed via reactive power injection/consumption, there is an increased reactive power flow via PCC, which might lead to additional costs for DSO (if a reactive power compensation market is enabled, however, that discussion is beyond this paper. Finally, the scenario LT.V shows a significantly reduced reactive power flow via PCC, which is a very positive consequence, as there is a capacity released at the distribution network providing a positive impact for the DSO, but in turn, this operation mode raises voltage fluctuations when compared to LT.IV. However, the voltage fluctuations are comparable to LT.II and less than in the case of LT.I.

Table 7. Summary of the simulation results with BESS of the long term operational scenarios.

OS	Short description	PCC Umax [p.u.]	PCC Umin [p.u.]	VD [%]	P DSO Import [MWh]	P DSO Export [MWh]	Q DSO Import [MVARh]	Q DSO Export [MVARh]	TSO Losses [MWh]	DSO Losses [MWh]
I	Initial	1.035042	0.9818979	5.31	64 395	-	10 252	740	87 230	209
II	PV+BESS const Q=0	1.035042	0.983184	5.19	38 683	13 366	10 242	717	87 219	149
III	Paper [AV8]	1.033343	0.9843438	4.90	38 686	13 364	17 131	-	87 231	154
IV	Station const U	1.031806	0.9861141	4.57	38 688	13 365	17 578	50	87 217	156
V	Station const Q	1.034645	0.9861058	4.85	38 729	13 344	220	5	87 184	143

6. CONCLUSIONS

Power electronic converters (PECs) have the potential to provide a wide variety of services when well-designed controllers and appropriate settings are used. The IEEE std.

1457-2018 provide the basis to enable the PECs with more active voltage control. Furthermore, several places worldwide are developing customer-centred legislation and markets; consequently, the smart inverters empower the DSO by creating positive TSO/DSO interactions. This research paper presents a comprehensive assessment of the steady-state performance of the DSO-TSO interaction caused by several voltage control strategies in smart-inverters installed at the DSO network. The assessment considers two different time scales: short term (24-hours, 1-minute resolution) and long-term (one-year) horizon. The three leading indicators are used in the assessment: total energy losses voltage profile in the TSO-DSO system and the power flow interaction at the interface between the systems. The assessment is based on numerical results using the DIgSILENT PowerFactory simulation tool, where the voltage controllers have been implemented, and regional electrical system in south-eastern Norway, the area of Vestfold and Telemark as been used for illustrative purposes. Overall results indicate that voltage profiles are improved when the smart converters work at constant voltage, and operation to constant reactive power provides a better reduction in total energy losses.

7. REFERENCES

[1] Thomas Krechel; F. Sanchez; F. Gonzalez-Longatt; H. Chamorro; Jose Luis Rueda, "Transmission System Friendly Micro-grids: An option to provide Ancillary Services", Distributed Energy Resources in Microgrids, Elsevier, 2018.

[2] P. Meraz et al., "Renewable Energy and Economic Dispatch Integration Within the Honduras Electricity Market", Springer, Singapore, 2021, pp. 1–34.

[3] F. S. Gorostiza, F. Gonzalez-Longatt, "Deep Reinforcement Learning-Based Controller for SOC Management of Multi-Electrical Energy Storage System", IEEE Transactions on Smart Grid, Vol. 3053, No. C, 2020, pp. 1–1.

[4] W. Cui, B. Zhang, "Lyapunov-Regularized Reinforcement Learning for Power System Transient Stability", IEEE Control Systems Letters, Vol. 6, 2022, pp. 974-979.

[5] IEEE PES Industry Technical Support Task Force, "Impact of IEEE 1547 Standard on Smart Inverters", 2018.

[6] D. Chathurangi, U. Jayatunga, S. Perera, A.P. Agalgaonkar; T. Siyambalapitiya, "Comparative evaluation of solar PV hosting capacity enhancement using Volt-VAr and Volt-Watt control strategies", Renewable Energy, Vol. 177, 2021, pp. 1063-1075.

[7] A. Perilla, J. L. Rueda Torres, S. Papadakis, E. Rakhshani, M. van der Meijden, F. Gonzalez-Longatt, "Power-Angle Modulation Controller to Support Transient Stability of Power Systems Dominated by Power Electronic Interfaced Wind Generation", Energies, Vol. 13, No. 12, 2020, p. 3178.

[8] P. Betancourt-Paulino, H. R. Chamorro, M. Soleimani, F. Gonzalez-Longatt, V. K. Sood, W. Martinez, "On the perspective of grid architecture model with high TSO-DSO interaction", IET Energy Systems Integration, Vol. 2021, 2020, pp. 1–12.

[9] T. Krechel, F. Sanchez, F. Gonzalez-Longatt, H. Chamorro, J. L. Rueda, "Transmission system-friendly microgrids: an option to provide ancillary services", Distributed Energy Resources in Microgrids, 2019, pp. 291–321.

[10] E. Rakhshani, A. Perilla, J. R. Torres, F. G. Longatt, T. B. Soeiro, M. Van Der Meijden, "FAPI Controller for Frequency Support in Low-Inertia Power Systems", IEEE Open Access Journal of Power and Energy, Vol. 7, 2020, pp. 276-286.

[11] D. Pettersen, E. Melfald, A. Chowdhury, M. N. Acosta, F. Gonzalez-Longatt, D. Topic", TSO – DSO Performance Considering Volt-Var Control at Smart-Inverters: Case of Vestfold and Telemark in Norway", 2020.

[12] A. Hirsch, Y. Parag, J. Guerrero, "Microgrids: A review of technologies, key drivers, and outstanding issues", Renewable and Sustainable Energy Reviews, Vol. 90, 2018, pp. 402–411.

[13] A. Peña Asensio, F. Gonzalez-Longatt, S. Arnaltes, J. L. Rodríguez-Amenedo, "Analysis of the Converter Synchronizing Method for the Contribution of Battery Energy Storage Systems to Inertia Emulation", Energies, Vol. 13, No. 6, 2020, p. 1478.

[14] F. Gonzalez-Longatt, J. L. Rueda, "Advanced Smart Grid Functionalities Based on PowerFactory", Springer, United Kingdom, 2018.

[15] Y. A. I. Mohamed, A. A. Radwan, "Hierarchical Control System for Robust Microgrid Operation and Seamless Mode Transfer in Active Distribution Systems", IEEE Transactions on Smart Grid, Vol. 2, No. 2, 2011, pp. 352-362.

[16] "TSO-DSO interaction: An Overview of current interaction between transmission and distribution system operators and an assessment of their cooperation in Smart Grids", 2014, https://smartgrids.no/wp-content/uploads/sites/4/2016/01/ISGAN-TSO-DSO-interaction.pdf (accessed: 2020)

[17] "Demand Connection Code." https://electricity.network-codes.eu/network_codes/dcc/ (accessed Oct. 13, 2018).

[18] J. Morin, F. Colas, X. Guillad, J.-Y. Dieulot, S. Grenard, "Joint DSO–TSO reactive power management for an HV system considering MV systems support", CIRED - Open Access Proceedings Journal, Vol. 2017, No. 1, 2017, pp. 1269–1273.

[19] H. R. Chamorro, I. Riaño, R. Gerndt, I. Zelinka, F. Gonzalez-Longatt, V. K. Sood, "Synthetic inertia control based on fuzzy adaptive differential evolution", International Journal of Electrical Power & Energy Systems, Vol. 105, 2019, pp. 803–813.

[20] P. Regulski, F. Gonzalez-Longatt, V. Terzija, "Estimation of load model parameters from instantaneous voltage and current", Proceedings of the IEEE International Conference on Fuzzy Systems, Taipei, Taiwan, 27-30 June 2011.

[21] R. Torkzadeh, H. R. Chamorro, R. Rye, M. Eliassi, L. Toma, F. Gonzalez-Longatt, "Reactive Power Control of Grid-Interactive Battery Energy Storage System for WADC", Proceedings of the IEEE PES Innovative Smart Grid Technologies Europe, Bucharest, Romania, 29 September - 2 October 2019.

[22] D. T. Rizy, Y. Xu, H. Li, F. Li, P. Irminger, "Volt/Var control using inverter-based distributed energy resources", Proceedings of the IEEE Power and Energy Society General Meeting, Detroit, MI, USA, 24-28 July 2011, pp. 1-8.

[23] F. Gonzalez-Longatt, B. S. Rajpurohit, S. N. Singh, "Optimal structure of a Smart DC micro-grid for a cluster of zero net energy buildings", Proceedings of the IEEE International Energy Conference, Leuven, Belgium, 4-8 April 2016, pp. 1–7.

[24] S. Mugemanyi, Z. Qu, F. X. Rugema, Y. Dong, C. Bananeza, L. Wang, "Optimal Reactive Power Dispatch Using Chaotic Bat Algorithm", IEEE Access, Vol. 8, 2020, pp. 65830-65867.

[25] "Power Generating Plants in the Low Voltage Network (VDE-AR-N 4105)." https://www.vde.com/en/fnn/topics/technical-connection-rules/power-generating-plants (accessed: 2021).

[26] Y. Bae, T. Vu, R. Kim, "Implemental Control Strategy for Grid Stabilization of Grid-Connected PV System Based on German Grid Code in Symmetrical Low-to-Medium Voltage Network", in IEEE Transactions on Energy Conversion, Vol. 28, No. 3, pp. 619-631, Sept. 2013.

[27] V. Astapov, P. H. Divshali, L. Söder, "The potential of distribution grid as an alternative source for reactive power control in transmission grid", Proceedings of the 19th International Scientific Conference on Electric Power Engineering, Brno, Czech Republic, 16-18 May 2018, pp. 1–6.

[28] M. Tomaszewski, S. Stanković, I. Leisse, L. Söder, "Minimisation of Reactive Power Exchange at the DSO/TSO interface: Öland case", Proceedings of the IEEE PES Innovative Smart Grid Technologies Europe, Bucharest, Romania, 29 September - 2 October 2019, pp. 1-5.

[29] H. Laaksonen, C. Parthasarathy, H. Khajeh, M. Shafie-Khah, N. Hatziargyriou, "Flexibility Services Provision by Frequency-Dependent Control of On-Load Tap-Changer and Distributed Energy Resources", IEEE Access, Vol. 9, 2021, pp. 45587-45599.

[30] M. N. Acosta, F. Gonzalez-Longatt, S. Denysiuk, H. Strelkova, "Optimal Settings of Fast Active Power Controller: Nordic Case", Proceedings of the IEEE 7th International Conference on Energy Smart Systems, Kyiv, Ukraine, 12-14 May 2020.

[31] M. N. Acosta, F. Gonzalez-Longatt, D. Topić, M. A. Andrade, "Optimal Microgrid–Interactive Reactive Power Management for Day–Ahead Operation", Energies, Vol. 14, No. 5, 2021, p. 1275.

[32] F. Gonzalez-Longatt; F. Sanchez; B. S. Rajpurohit; S. N. Singh, R. K. Chuahan, "On Topology for a Smart DC micro-grid for a Cluster of Zero Net Energy Buildings", Distributed Energy Resources in Microgrids, Elsevier, 2019.

[33] I. Richardson, M. Thomson, D. Infield, "A high-resolution domestic building occupancy model for energy demand simulations", Energy and Buildings, Vol. 40, No. 8, 2008, pp. 1560-1566.

[34] A. Sharma, M. Kolhe, S. O. Kristiansen, S. Simonsen, H. Landsverk, S. M. Oland, "Techno-Economic Case Study of Micro-Grid System at Soccer Club of Skagerak Arena Norway", Proceedings of the 2020 5th International Conference on Smart and Sustainable Technologies, Split, Croatia, 23-26 September 2020, pp. 1-5.

[35] K. Berg, M. Resch, T. Weniger, S. Simonsen, "Economic evaluation of operation strategies for battery systems in football stadiums: A Norwegian case study", Journal of Energy Storage, Volume 34, 2021.

[36] A. Eid, A. Y. Abdelaziz, M. Dardeer, "Energy Loss Reduction of Distribution Systems Equipped with Multiple Distributed Generations Considering Uncertainty using Manta-Ray Foraging Optimization", International Journal of Renewable Energy Development, Vol. 10, No. 4, 2021, pp. 779-787.